Colloid Polym Sci (2009) 287:671–681
DOI 10.1007/s00396-009-2026-z

ORIGINAL CONTRIBUTION

Poly(L-lactide) networks with tailored water sorption

Jorge Luis Escobar Ivirico · Manuel Salmerón-Sánchez · José Luis Gómez Ribelles · Manuel Monleón Pradas

Received: 10 November 2008 / Accepted: 23 March 2009 / Published online: 14 April 2009
© Springer-Verlag 2009

Abstract A poly(L-lactide) diol was obtained through ring opening polymerization of L-lactide, using 1,6 hexanediol and tin(II) 2 ethylhexanoate as a catalyst. In the second step, the poly(L-lactide) macromer (mLA) was obtained by the reaction of poly(L-lactide) diol with methacrylic anhydride. The effective incorporation of the polymerizable end groups was assessed by Fourier transform infrared spectroscopy and nuclear magnetic resonance (^{1}H NMR). Besides, poly(L-lactide) networks (pmLA) were prepared by photopolymerization of mLA. Further, the macromer was copolymerized with 2-hydroxyethyl acrylate seeking to tailor the hydrophilicity of the system. A set of hydrophilic copolymer networks were obtained. The phase microstructure of the new system and the network architecture was investigated by differential scanning calorimetry, infrared spectroscopy, dynamic mechanical spectroscopy, thermogravimetry, and water sorption studies.

Keywords Hydrogels · Macromers · *p*(L-Lactide) diol · Copolymer networks

J. L. Escobar Ivirico (✉) · M. Salmerón-Sánchez · J. L. Gómez Ribelles · M. Monleón Pradas
Center for Biomaterials and Tissue Engineering,
Universidad Politécnica de Valencia,
46022 Valencia, Spain
e-mail: joresciv@ter.upv.es

M. Salmerón-Sánchez · J. L. Gómez Ribelles · M. Monleón Pradas
Centro de Investigación Príncipe Felipe,
Autopista del Saler 16,
46013 Valencia, Spain

J. L. Escobar Ivirico · M. Salmerón-Sánchez · J. L. Gómez Ribelles · M. Monleón Pradas
Networking Research Center on Bioengineering,
Biomaterials and Nanomedicine (CIBER-BBN),
46022 Valencia, Spain

Introduction

Tissue engineering employs the principles and methods of engineering, biology, and medicine toward the development of biological substitutes that restore, maintain, or improve function in normal or pathological tissue or organs [1]. A number of tissues and organs have been extensively investigated by this approach, e.g., cartilage, skin, liver, bone, etc. Polymeric materials play an important role in tissue engineering and are being applied in conducting, guiding, and inducing tissue formation [2–6]. Biodegradable polyesters and copolyesters have been the focus of extensive research for several decades as a result of their easy manufacturing and desirable characteristics. Among the polyesters, the polymers derived from α-hydroxy acids (lactic acid and glycolic acid) have found the most extensive use [7, 8] primarily as materials for sutures dating back to the early 1960s due to their superior biocompatibility and acceptable degradation profiles [9]. Poly(L-lactide) (PLLA) has attracted much attention as a biodegradable thermoplastic polymer since it has excellent biocompatibility, suitable physical properties, is available from renewable sources, and degrades completely to non-toxic water and carbon dioxide in vitro and lactic acid in vivo [10]. Biodegradable cross-linked PLLA has been the focus of some researcher groups, seeking to provide PLLA with different characteristics in regard to thermoplastic biopolymers. With this aim, new synthetic routes to biodegradable materials have been recently opened [11–17]. Thus, PLLA and its copolymers have been widely studied for a variety of biomedical applications.

Hydrophilicity is one of the properties that determine the spectrum of applications of a biomaterial. For example, the adhesion and growth of cells on a surface are considered to be strongly influenced by the balance of hydrophilic and hydrophobic groups, frequently described

as wettability even if the concept it is not the same [18–20]. Different procedures to graft hydrophilic groups on a hydrophobic surface and control their amount and distribution can be found in the literature by ammonia or sulfur dioxide plasma treatments [21, 22], by irradiation, by photo- or plasma-induced grafting of hydrophilic polymers [23–26], as well as by ion implantation treatment [27, 28]. With the same aim, blending of PLLA with hydrophilic polymers has been reported, e.g., Langer et al. [29] have prepared poly(L-lactide)/pluronic blends as protein-releasing matrices. On another hand, cross-linking is another way of modifying the microstructure and some key physicochemical properties of a polymer. This is the case of poly(D,L)-lactide macromer copolymerized with 2-hydroxyethylmethacrylate, getting an increase of swelling degree with hydrophilic monomer content increment and also their effect (hydrophilic/hydrophobic ratios) under the drug controlled release [30]. By hydrophilizing and cross-linking PLLA physical properties such as crystallinity, melting point, glass transition temperature, thermal degradation, mechanical properties, solubility, and others are modified affecting in the end the biodegradability of the material.

In this work, we aim at preparing a new family of materials that must lead in the future to the preparation of porous scaffolds for tissue engineering. The new system must keep excellent PLLA properties such as biocompatibility and biodegradability, but the hydrophilicity of the system can be tailored in an independent way. For that, we obtain a L-lactide macromer through condensation of poly(L-lactide) diol with methacrylic anhydride to get methacrylate endcapped PLLA able to self-cross-linking. The resulting macromer was assessed by Fourier transform infrared spectroscopy (FTIR) and ^{1}H NMR. PLLA networks were prepared by photopolymerization of the new macromer. The PLLA macromer was copolymerized with 2-hydroxyethyl acrylate in different proportions to give copolymer networks with the aim of modulating the water sorption capacity of the system. The structure and properties of the new system were assessed by differential scanning calorimetry (DSC), thermogravimetric analysis (TGA), dynamic mechanical spectroscopy (DMS), and water sorption ability.

Experimental

Materials

L-Lactide, 1,6 hexanediol, tin(II) 2 ethylhexanoate, methacrylic anhydride, and 2-hydroxyethyl acrylate (HEA) were supplied by Aldrich. Benzoin (Scharlau 98% pure) was employed as initiator. Dioxane (Aldrich, 99.8% pure), acetone (Aldrich, 99.5% pure), ethanol (Aldrich, 99.5% pure), and ethyl acetate anhydrous (Aldrich 99.8%) were used as solvents. Distilled water with 10 μS conductivity was used in the swelling studies.

Preparation of α,ω-hydroxyl terminated poly(L-lactide)

Poly(L-lactide) diol (macromer diol) was prepared by the synthesis of L-lactide with 1,6 hexanediol as follow. In a 50-ml three-neck round bottom flask, 0.409 g of 1,6 hexanediol, 10 g of L-lactide (20 mol of L-lactide/mol of hexanediol), 21 mg of tin(II) 2 ethylhexanoate, and 2 ml of methylene chloride were charged. The reaction mixture was melted by heating to 90°C. When most of the solvent had evaporated, the system was stirred under vacuum at 180°C for 5 h and cooled at room temperature under slow stirring. The resulting macromer diol (yield 85%) was dissolved in acetone and precipitated in ethanol, filtrated, and dried. The α- and ω-hydroxyl groups of poly(L-lactide)-diol were used in the preparation of poly(L-lactide) macromer. The molecular weight was determined by NMR analysis.

Synthesis of methacrylate-endcapped poly(L-lactide) macromer

The α- and ω-dihydroxyl terminated poly(L-lactide) was endcapped with methacrylate groups to obtain a macromer, which could undergo radical polymerization. Briefly, 10 g of poly(lactide) diol (M_n=3,500 Da) was dissolved in 50 ml ethyl acetate anhydrous in a 100-ml three-neck flask and react with a 20-fold excess of methacrylic anhydride under stirring at 0°C for 1 h and after at 80°C for 8 h under N_2 (g) atmosphere. The reaction was followed by thin layer chromatography. The macromer was obtained by dropping the filtrate into an excess of ethanol, filtrated, recrystallized for several times in ethanol to purify the white solid, and also purified again by column chromatography techniques, using silica gel 60 (70–230 μm mesh) as stationary phase and ethyl acetate as solvent. Finally, the precipitated poly(L-lactide) macromer was dried at 60°C for 24 h under reduced pressure. The molecular weight was determined by NMR analysis.

Poly(L-lactide) networks

Poly(L-lactide) networks were prepared by UV polymerization. The poly(L-lactide) macromer was dissolved in dioxane, 35% (*w*/*v*) and mixed with benzoin (photoinitiator, 1 wt.%). The reaction was carried out in ultraviolet light for 24 h. Low molecular weight substances were extracted by boiling in ethanol for 24 h and then drying in a vacuum to constant weight.

Poly(L-lactide) copolymer networks

The self-cross-linked copolymer networks with different compositions of both monomers (see Table 1, molar ratio of mLA and HEA) were synthesized by radical copolymerization in solution using dioxane as solvent 35% (*w*/*v*) and benzoin as photoinitiator at 1 wt.%. The reaction was carried out in ultraviolet light for 24 h. Low molecular weight substances were extracted by boiling in ethanol for 24 h and then drying in a vacuum to constant weight (Appendix).

NMR spectroscopy

The structural characterization of the poly(L-lactide) diol and poly(L-lactide) macromer was conducted by NMR spectroscopy. The ^{1}H NMR spectra were obtained on a Bruker AMX operating at 500 MHz for protons. Both compound poly(L-lactide) diol and the macromer samples were prepared as 0.5% (*w*/*w*) solutions in $CDCl_3$ for NMR measurements, using tetramethylsilane as internal standard. All the chemical shifts for resonance signals are reported in parts per millions (ppm).

Attenuated total reflection Fourier transforms infrared spectroscopy (ATR-FTIR)

Attenuated total reflection Fourier transforms infrared spectroscopy (ATR-FTIR) spectra of each sample were generated by a Thermo Nicolet Nexus *FTIR* spectrophotometer, controlled by OMNIC software. The spectra were obtained by accumulating 64 scans in the range 650–4,000 cm^{-1} with a resolution of 4 cm^{-1}.

Differential scanning calorimetry

DSC was performed in a Mettler Toledo 823e apparatus. Nitrogen gas was purged through the DSC cell with a flow rate of 20 ml/min. The temperature of the equipment was calibrated by using indium and zinc. The melting heat of indium was used for calibrating the heat flow. After erasing the effects of any previous thermal history by heating to 200°C, the samples were subjected to a cooling scan down to −100°C at 10°C/min, followed by a heating scan from that temperature up to 200°C at a rate of 10°C/min. Samples were used as obtained weighting between 5 and 10 mg of each material.

Table 1 Network parameters

ω_{HEA}	n_{HEA}/n_{PCL}	MPHEA	M	E' (MPa)	M_c
0	0	–	–	0.30	14,795
0.3	13	750	1,667	2.10	2,250
0.5	30	1,750	2,333	2.50	1,874
0.7	70	4,083	3,889	1.20	3,993

Molar ratio HEA/mLA in the network (n_{HEA}/n_{PCL}); stoichiometric molar mass of PHEA between cross-links (M_{PHEA}); average molar mass between cross-links (M); measured storage modulus at 175°C (E); average molar mass between cross-links as calculated from rubber elasticity (M_c)

Dynamic mechanical analysis

Dynamic mechanical analysis (DMA) was performed in a Seiko DMS210 apparatus at a frequency of 1 Hz in the tension mode. The temperature dependence of the storage modulus and loss factor was measured in the temperature range from −100°C to 150°C at a rate of 2°C/min. Samples for DMA were prismatic and were cut from plates obtained after synthesis ($10\times4.5\times1$ mm^3).

Thermogravimetric analysis

Measurements were performed using a TA-Instruments Model SDT-Q600 system. Samples (5–10 mg weight) were placed on the balance, and the temperature rose from 50°C to 750°C at a heating rate of 10°C/min. The mass of the sample pan was continuously monitored as a function of temperature.

Swelling experiments

The swelling degree w was determined gravimetrically. Dry disks (5±0.05 mm diameter and 1±0.05 mm thickness) were prepared from polymerized sheets. Swelling experiments were performed by equilibrating the xerogels (dry disks) in distilled water at 37.0±0.1°C. The swelling degree w is expressed as the amount of water per unit mass of the dry polymer (xerogel):

$$w = \frac{m_{water}}{m_{xerogel}} \quad (1)$$

Density measurements

The densities of all networks were determined weighting the samples in air and immersed in *n*-octane as follow:

$$\rho_{sample} = \frac{m_{air}}{m_{air} - m_{solvent}} * \rho_{solvent} \quad (2)$$

where m_{air} and $m_{solvent}$ are the weight of the sample in air and in the solvent, respectively.

Results

Self cross-linkable L-lactide macromer (mLA)

α-ω-dihydroxyl terminated poly(L-lactide) was obtained by ring opening polymerization using tin(II) 2 ethylhexanoate as a transesterification catalyst [31–33] as we describe in the "Experimental" section.

Alkanediol initiator results in the formation of symmetrical macromer lactide diol having alkane cores and terminal hydroxyl groups. The synthesis of poly(L-lactide diol) was found to be sensitive to reaction temperature, resulting in very low product yield at temperatures lower than 180°C [34, 35]. On the other hand, the molecular weight and the monomer conversion increase with the polymerization time in initials stages, suggesting that ring opening polymerization of L-lactide proceeds not only by a chain reaction but also by a step-growth reaction mechanism. Suong-Hyu and coworkers [35] reported that the monomer conversion and molecular weight for L-lactide at the initial stages present a linear increase with time of reaction (about 80%) followed by a gradual decrease in both factors. The authors found that at 5 h and 180°C the monomer conversion keeps already the 80% and we select this procedure. As shown in Fig. 1, 1,6 hexanediol was used to initiate the polymerization of L-lactide monomer in the presence of tin(II) 2 ethylhexanoate catalyst to produce the poly(L-lactide) diol. The obtained polymer was dissolved in acetone and dropped into a mixture of ethanol and hydrochloric acid to assure the complete exchange of residual catalytic end group to hydroxyl functionality.

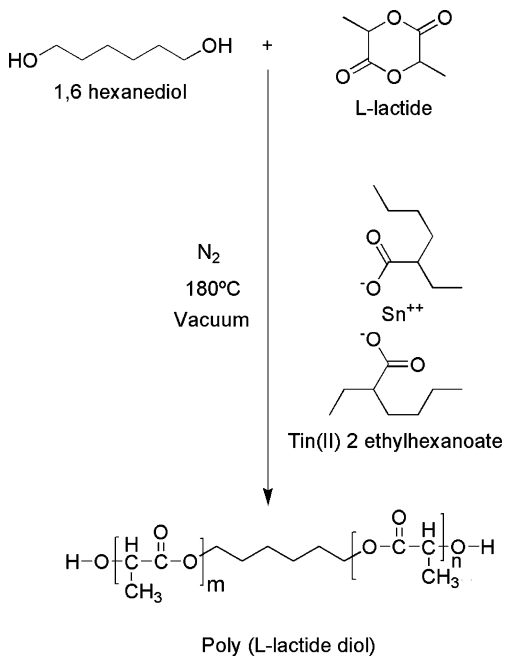

Fig. 1 Synthesis of poly(L-lactide) diol

Afterward, the α-ω-dihydroxyl terminated polymer was endcapped with methacrylic anhydride groups to make a self-cross-linkable macromer as we describe in Fig. 2.

A typical FTIR spectrum of poly(L-lactide) diol and poly (L-lactide) macromer is shown in Fig. 3. The absorption bands in the 3,600 to 3,300 cm^{-1} range associated to alcohols (OH stretching vibrations) for poly(L-lactide) diol vanish in the lactide macromomer (mLA) due to the esterification reaction. Other important modifications in the mLA spectrum compared with the poly(L-lactide) diol are the absorption bands at 1,640 cm^{-1} assigned to the C=C stretching vibrations due to methacrylation of poly(L-lactide) diol (note the arrow in Fig. 3). These bands were not observed in the original poly(L-lactide) diol. Significant signals are also the band located at 1,758 cm^{-1}, corresponding to the C=O stretch from lactidyl moieties of carboxyl group and that located at approx. 2,980–2,920 cm^{-1} due to the symmetrical and anti-symmetrical CH_3 and CH_2 stretching, which are present in both the poly (L-lactide) diol and poly(L-lactide) macromer.

The esterification signals were also clearly evident when comparing the ^1H NMR spectrum of poly(L-lactide) diol with that of the lactide macromer (Fig. 4). The spectrum for L-lactide macromer (mLA) shows, in addition to the signals already assigned in the poly(L-lactide) diol spectrum (Fig. 4a), the presence of new signals: two bands located at 6.21 and 5.80 ppm attributable to the vinyl CH_2 (j and i) of the methacrylic groups and a singlet at 2.00 ppm attributable to the CH_3 (h) of the methacrylic group. The poly(L-lactide) diol molar mass estimated to be 3,500 Da was determined using the integrals of the ^1H NMR spectra. The degree of modification was determined from the relative integrations of the methacrylate to poly(L-lactide) diol protons. The yield of the esterification reaction was calculated to be approximately 75%. The remaining (non-reacted) 25% is not observed in the spectrum since the macromer obtained from synthesis was purified by column chromatography before NMR measurement.

Poly(L-lactide) copolymer networks, *p*(mLA-co-HEA)

Radical polymerization of the obtained macromer (mLA) gives rise to the formation of polymer networks (Fig. 2). Moreover, different proportions of 2-hydroxyethyl acrylate were added as reactive so as to get copolymer networks, *p*(mLA-co-HEA). The ATR-FTIR spectra of the poly(L-lactide) network and its copolymer networks are shown in Fig. 5. The band at 3,600–3,200 cm^{-1} due to C–O–H stretching of the hydroxyl group increases with HEA content in the feed mixture. Significant signals are also the band located at 1,727 cm^{-1}, corresponding to the C=O

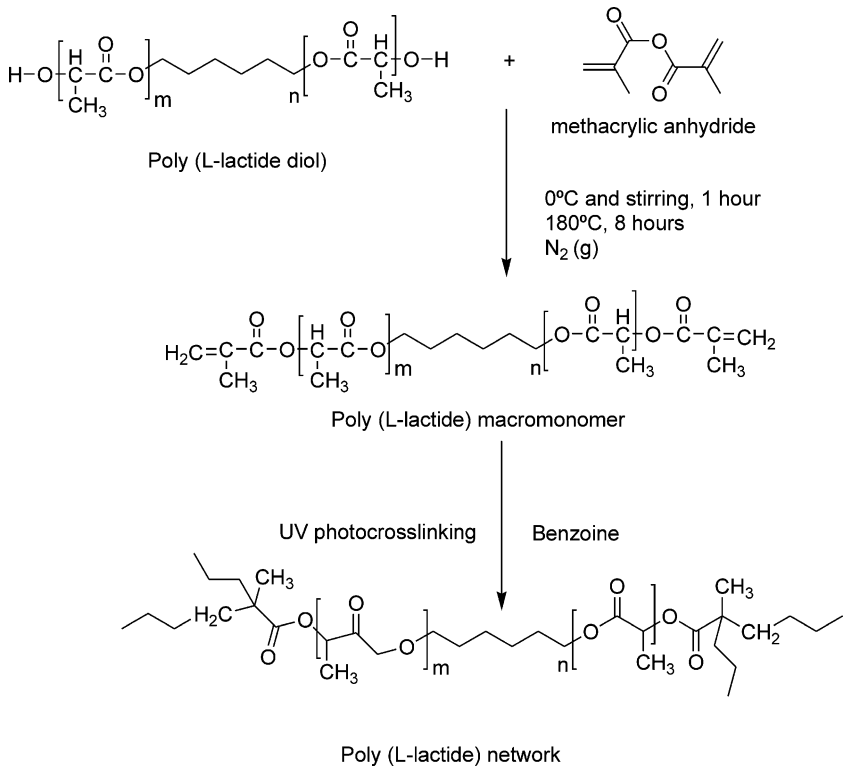

Fig. 2 Synthesis of self cross-linkable poly(L-lactide) macromer

stretching vibration of carboxyl group and that located at approx. 2,973–2,868 cm^{-1} due to the symmetrical and anti-symmetrical CH_3 and CH_2 stretching.

Figure 6 shows the DSC thermograms of the poly(L-lactide) diol, poly(L-lactide) macromer, the *p*(mLA-co-HEA) networks, and PHEA network. After erasing the effect of any previous thermal history by heating at 200°C for 3 min and cooling at 40°C/min to −100°C, DSC heating scans was measured from −100°C to 200°C. DSC curves show firstly for poly(L-lactide) diol and lactide macromer (mLA) the glass transition process around 40°C, followed by a crystallization exotherm (around 95°C) and the melting endotherm. Only the glass transition is observed for the homopolymer networks at approx. 50°C for the *p*(mLA) network and at 10°C for the PHEA network. The glass transition process for the copolymer networks seems to be the superposition of two processes located between those of the corresponding homonetworks. No crystallization process was detected in the DSC cooling thermogram at 10°C from the melt for any network.

TGA curves show the thermal degradation process of our system (Fig. 7). No weight loss has been detected below 230°C in any sample. The thermal degradation starts for poly (L-lactide) diol around 250°C and for poly(L-lactide) macromer around 300°C, reflecting the chemical differences in the structure between both compounds. On the other hand, poly (L-lactide) networks and poly(mLA-co-HEA) copolymers start degrading around 300°C. Degradation curves for the copolymer networks are located between those of the pure homopolymers. The rate of weight loss is better appreciated in a plot of the weight loss derivative versus temperature curve. We use the maxima in these plots to characterize different stages in the degradation process. The temperatures at which these maxima occur correspond to the temperatures at which the degradation process is faster. Thus, the loss of weight of the *p*(mLA) network is seen to proceed in three stages, which we call λ_1(325°C), λ_2(410°C), and λ_3 (500°C); that of PHEA proceeds in three stages χ_1(390°C), χ_2(450°C),

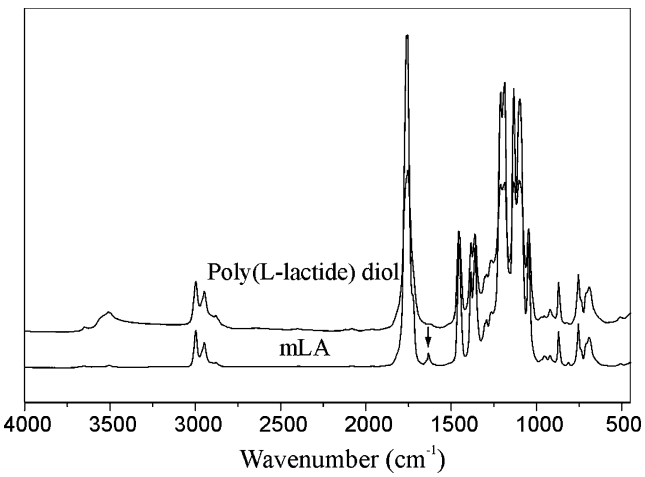

Fig. 3 ATR-FTIR spectra of poly(L-lactide) diol and methacrylate-encapped L-lactide macromer (mLA)

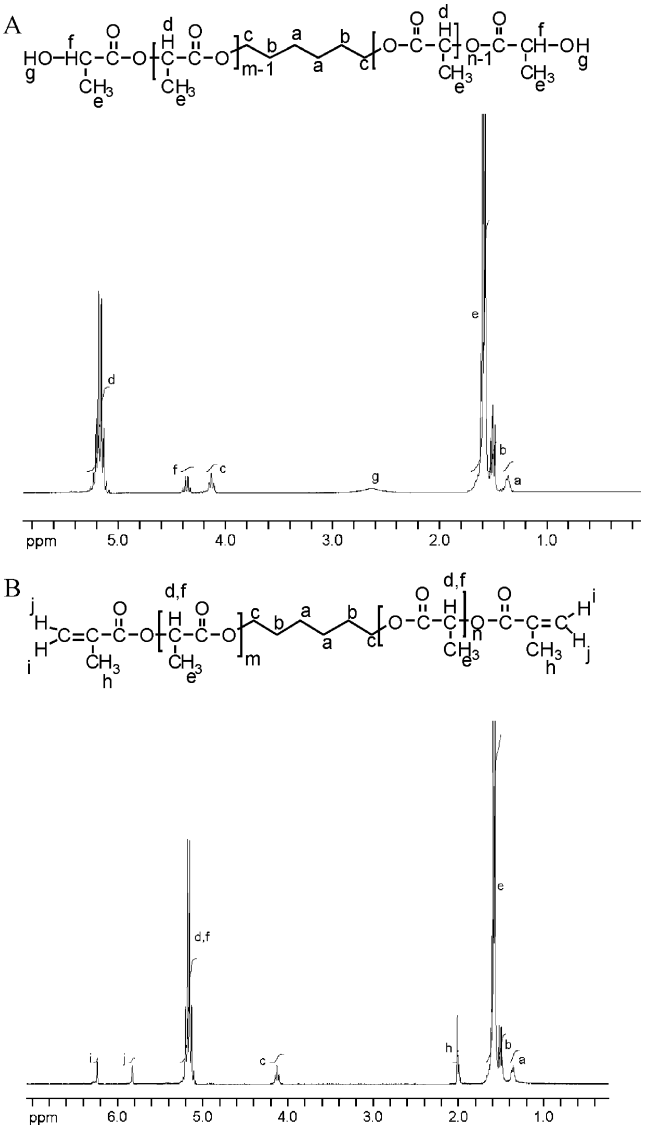

Fig. 4 ^{1}H NMR (500 MHz, $CDCl_3$) spectra of the **a** poly(L-lactide) diol and **b** methacrylate-endcapped lactide macromer (mLA)

and χ_3 (535°C). Three degradation stages can be identified for the copolymer networks: ξ_1(325°C), ξ_2(450°C), and ξ_3(535°C) whose temperature (ξ_2 and ξ_3) depends slightly on the weight fraction x of HEA in the sample.

Figure 8 shows the mechanical storage modulus and the loss angle tangent of the copolymer networks. At the highest temperatures of the scan, the elastic modulus remains stable, which is characteristic of the network structure.

The rubbery modulus is approx 10^5 Pa for the *p*(mLA) network, and it increases as the HEA content in the system does. The main relaxation is very broad (it ranges from 30°C to 100°C) for the *p*(mLA) network and is steeper and located at 25°C for the PHEA network. The main relaxation process for the copolymer networks is very broad and located between those of the homopolymers. Moreover, the temperature dependence of the modulus shows a splitting into two

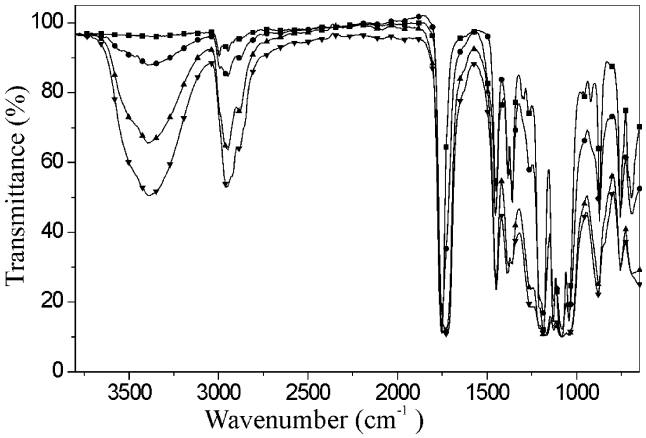

Fig. 5 ATR-FTIR spectra of *p*(mLA) (*squares*) and the copolymers containing 30% HEA (*circles*), 50% HEA (*triangles*), and 70% HEA (*inverted triangles*)

drops as the HEA content increases. The final drop in pmLA modulus (from 100°C to 150°C) is due to the melting of the crystal phase present in the as synthesized sample.

Figure 9 shows the specific volume of the copolymer networks as calculated from the density measurements. As we can see, a decrease tendency with the increment of HEA content (not lineal dependence) was found.

Figure 10 represents the gain of weight of the samples after immersion in distilled water, w (Eq. 1) and also the amount of water sorption by the HEA unit (w') in the copolymers.

$$w' = \frac{w - w_{\mathrm{mLA}}(1 - \omega_{\mathrm{HEA}})}{\omega_{\mathrm{HEA}}} \tag{3}$$

where w_{mLA} is the sorption capacity of the *p*(mLA) network. This magnitude is composition dependent, and it never reaches the value of the equilibrium water sorption for the PHEA homonetwork. This discrepancy again reinforces the idea that the HEA units in the copolymer have molecular environments different from those they have in a homogeneous PHEA phase. Nevertheless, the steady increase in w'

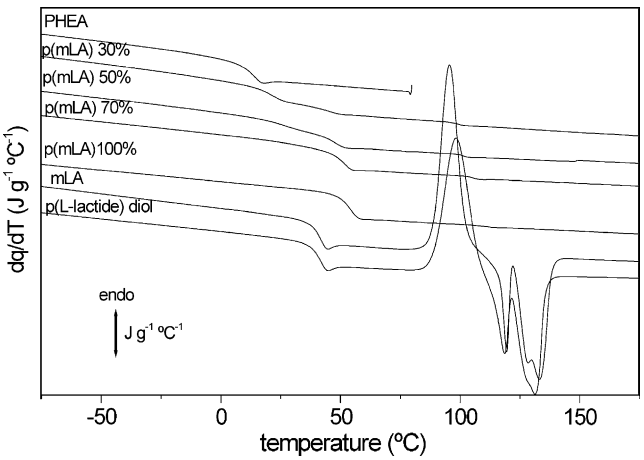

Fig. 6 DSC heating curves at 10°C/min

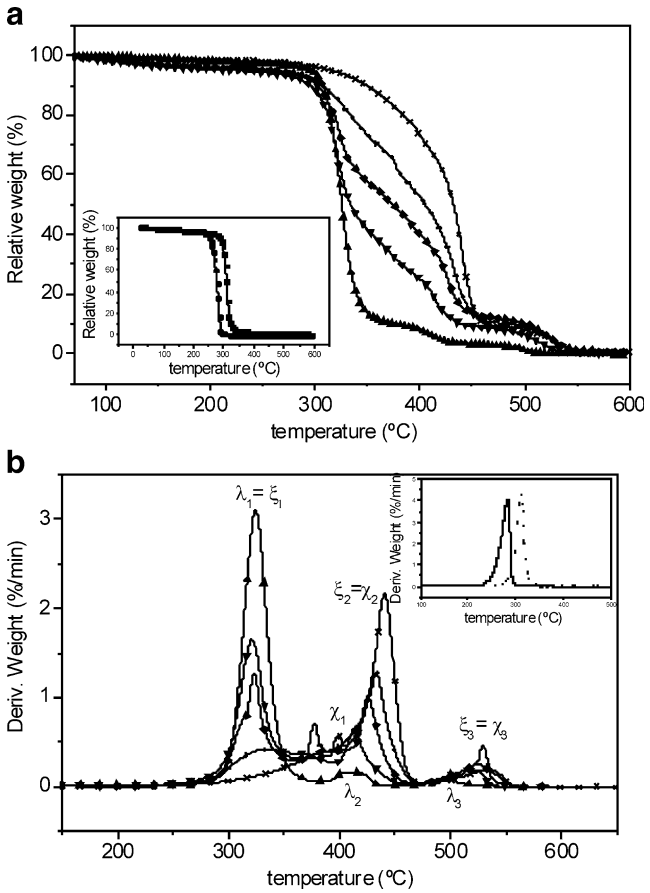

Fig. 7 Thermogravimetry of poly(L-lactide diol) (*squares* in the *inset*), poly(L-lactide) macromer (*circles* in the *inset*), *p*(mLA) (*triangles*), PHEA (*multiplication signs*), and the copolymers containing 30% HEA (*inverted triangles*), 50% HEA (*diamonds*), and 70% HEA (*plus signs*). The relative weight loss (**a**) and the derivate of the weight loss versus the temperature (**b**) are shown for all samples

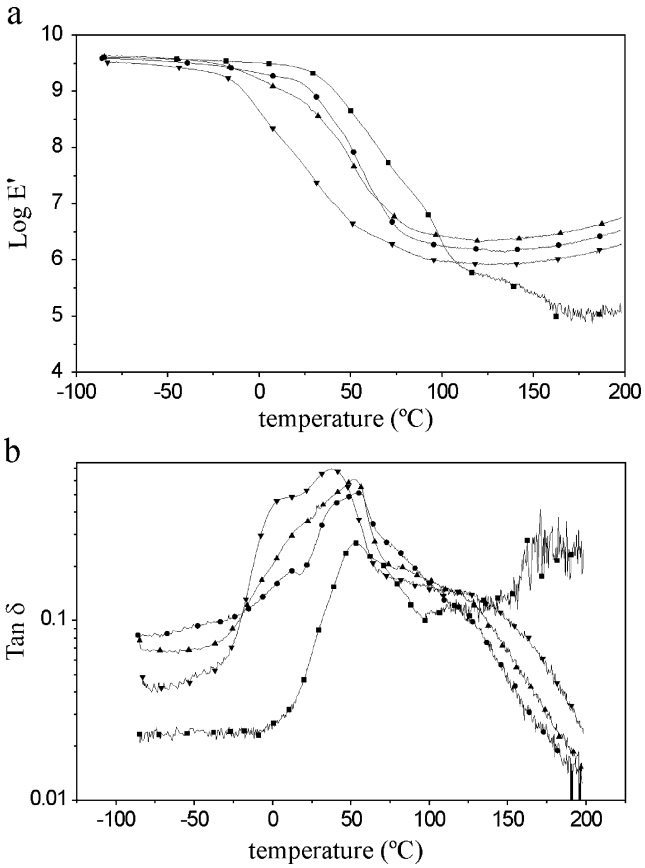

Fig. 8 Dynamic storage modulus (log *E*′) and the loss tangent measured on heating. *p*(mLA) (*squares*) and the copolymers: 30% HEA (*circles*), 50% HEA (*triangles*), 70% HEA (*inverted triangles*)

revealed in Fig. 10 suggests that the HEA-rich nanodomains are more and more pure (less mLA chains included) as the HEA content in the copolymer increases. This behavior was also found for other polyester for example a different chemical modification of polycaprolactone copolymerized with HEA units [36, 37].

Discussion

Poly(L-lactide) diol was successfully endcapped with methacrylate groups to give L-lactide macromer able to self-cross-linking following the route sketched in Figs. 1 and 2. The structures were characterized by FT-IR and ^{1}H NMR (Figs. 3 and 4). The fuctionalization degree (FD) was estimated by ^{1}H NMR through the relative intensity of the signal of CH_2 (c) and one of the vinyl CH_2 (j or i) group that are expected to be the same for a 100% FD. The FD thus estimated was ≈75%. The incorporation of methacrylate groups allows the photo-cross-linking of the system.

Polymer networks based on the lactide macromer and a hydrophilic monomer, HEA, were prepared in the whole composition range of both comonomers. The absence of any loss of weight before 200°C (Fig. 7) assesses the effective incorporation of HEA units into the polymer chains discarding the presence of residual HEA in the samples; had unreacted

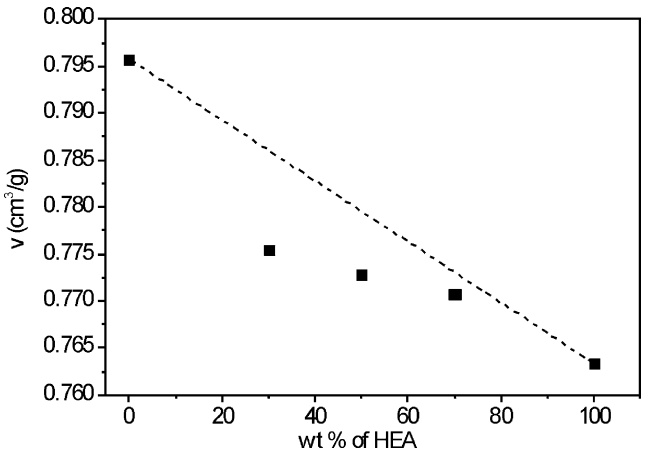

Fig. 9 Specific volume of *p*(mLA), PHEA, and the copolymer networks as a function of the HEA mass fraction in the copolymer

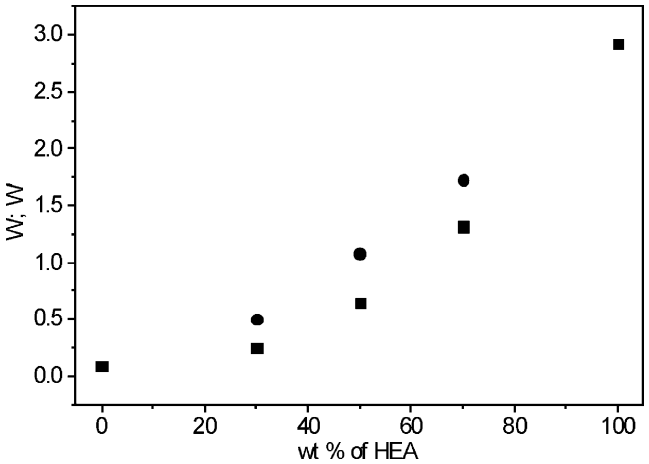

Fig. 10 Equilibrium water content (*w*, *squares*) per unit mass of sample and per unit mass of HEA unit in the copolymer (*w'*, *circles*)

monomer been present, the thermograms would have shown a weight loss as a consequence of the evaporation of the HEA monomer at much lower temperatures.

The weight loss derivative curve shows how the peak located at 450°C is displaced to lower temperatures as the HEA content of the copolymer decreases. When the temperature interval of the main degradation stage of PHEA, (stage χ_2) that has been ascribed to the degradation of the acrylate main chain, is attained in the heating scan of a copolymer, most of the *p*(mLA) chains have already disappeared since more than 90% of the weight of *p*(mLA) is lost below 350°C, in the λ_1 stage of pure *p*(mLA) or ξ_1 stage in the copolymers, which must imply the degradation of the polylactide chains. Thus, one may hypothesize that the ξ_2 stage in the copolymers is due to the degradation of the acrylate chains that shifts toward lower temperatures as the HEA content increases. In fact, the χ_2 process of PHEA takes place at higher temperatures than the λ_2 stage of pure *p*(mLA).

The ratio of HEA units per mLA macromer unit can be stoichiometrically estimated as

$$\frac{n_{\mathrm{HEA}}}{n_{\mathrm{mLA}}} = \frac{\omega_{\mathrm{HEA}}}{1-\omega_{\mathrm{HEA}}}\frac{M_{\mathrm{mLA}}}{M_{\mathrm{HEA}}} \tag{4}$$

where *n* is the mol number, ω_{HEA} is the mass fraction of HEA in the system, and *M* is the molar mass. Table 1 shows the calculated values for the different copolymer networks using Eq. 4. The molecular architecture of the copolymer network depends on the way in which these HEA units are incorporated within the system during the copolymerization reaction. The calculation of mass fraction of HEA in the systems was performed assuming full conversion in the polymerization process. It is known that radical polymerization usually leads to very high yielding (above 90%). Tutusaus and coworkers found the very highly efficient catalyst of some precursors for the controlled radical polymerization of styrene and *n*-butyl acrylate, getting polymers yields about 90% [38]. Kanaoka et al. employed cationic polymerization to prepare core cross-linked star polymers in high yield via the cross-linking of living poly (*iso*butyl vinyl ether) with divinyl ether cross-linkers [39].

The specific volume of the copolymer networks (Fig. 9) decreases as the amount of HEA in the system increases but the values do not depend linearly on the weight fraction of HEA in the copolymer. As a fact, they fall below the straight line that joints the values corresponding to homopolymer networks, i.e., the steric arrangement of the chains in the copolymer is such that it leads to a better packing (less free volume) than in the case of the homopolymers, which preserve their free volume in ideal mixtures. This departure from thermodynamical ideality is due both to steric reasons and to the occurrence of specific interactions intraspecies. In our case, these can be detected by DSC as a modification of the glass transition processes in the copolymer networks. It is worth noting that crystallization of L-lactide units that takes place in poly(L-lactide) diol and poly(mLA) and also in conventional poly (L-lactide) [40] is prevented in the *p*(mLA) network by the topological constraints imposed by the network structure. On another other hand, polymer networks based on polycaprolactone diol with molecular weight 2,000 Da showed some crystallinity [36]. The much slower crystallization rate of PLLA with respect to PCL [41] can explain this different behavior and perhaps long annealing times at temperatures in the range immediately below the endotherm shown in the DSC heating scans by poly(L-lactide) diol and poly(mLA) could induce some crystallinity in *p*(mLA) networks and eventually in high mLA content copolymers. But, with the thermal histories of the experiments of this work, pmLA and the copolymer networks are fully amorphous. The glass transition temperature of the *p*(mLA) network is located at approx. 45°C. If ω_{HEA} in the network is 0.3, T_g of the mLA chains is moved to lower temperatures (to approximately 40°C), and there is no detectable trace for the glass transition process of the HEA units. For higher amounts of HEA in the system (ω_{HEA}=0.5), a double glass transition appears, the higher temperature transition in the temperature range of that of *p*(mLA) shifted toward lower temperatures, while the lower temperature one is identified at approx. 25°C, which is in the range of the glass transition of HEA units but at higher temperatures than the T_g of the PHEA network. Higher amounts of HEA in the system (ω_{HEA}=0.7) give rise again to a double glass transition process. The one at higher temperatures, assigned to the mLA chains, takes place at the same temperatures as the glass transition of the mLA units in the system with ω_{HEA}= 0.5, and the second one, associated to HEA domains, takes place still at higher temperatures than the glass transition of the PHEA homonetwork (but lower than the corresponding one in the ω_{HEA}=0.5 system).

The DMS in Fig. 8 shows a single relaxation process for the *p*(mLA) networks, which is ascribed to the main α_{mLA} relaxation. The main relaxation process splits into two subprocesses as the amount of HEA in the system increases (Fig. 8b). The peak at lower temperature is related to the α relaxation of the hydrophilic of HEA units (α_{HEA}): the higher the magnitude, the higher the fraction of HEA in the copolymer network. The broadness and temperature position of the peaks reveal the influence of one component on the other. The α_{HEA} process moves to lower temperatures as the amount of HEA in the system increases. In the same sense, the α_{mLA} process moves to higher temperatures the lower the fraction of HEA in the system is. Moreover, the magnitude of the relaxation peaks in the copolymer—compared to that of the α_{mLA} relaxation for the lactide macromer—reveals the heterogeneity in composition of the domains, which gives rise to the relaxation process.

Both DSC and DMS results reveal features of the phase microstructure of the copolymer networks. For HEA fractions in the system ω_{HEA} lower than 0.3, that is, approx. 13 HEA units per mLA chain, the system consists of mLA chains plasticized by the HEA units. There are no pure HEA domains big enough such as to give an independent glass transition process by DSC. Higher amounts of HEA in the system, from ω_{HEA}=0.5 on, give rise to the formation of two kind of domains, each one richer in one or the other comonomer; a fraction of the HEA units still plays the role of a plasticizer of the mLA chains—the glass transition process moves to lower temperatures—but the rest are able to reorganize by cooperative rearrangements that give rise to HEA glass transition observed by DSC. As the amount of HEA increases, ω_{HEA}=0.7, the additional HEA units do not plasticize further the mLA rich phase and the T_g of the mLA chains stabilizes, which suggests that no more than 30 units of HEA per mLA chain (see Table 1) are able to interact with mLA chains at the distance of the cooperative rearranging region at T_g (a few nanometers), and the rest, i.e., 40 HEA units per mLA chains (Table 1), constitute an aggregate big enough such as to give rise to an independent glass transition process. These domains, however, are not entirely pure PHEA domains since the temperatures of the glass transitions show that some mLA chains must be included in them (Fig. 6).

The *p*(mLA) network is formed from a tetrafunctional macromer (Fig. 2). To these elements, the copolymers add units of linear HEA monomer (116 g mol^{-1}) in the proportions shown in Table 1. The topology of the resulting copolymerized network can be ideally thought to be that sketched in Fig. 11, with a number of monomeric HEA units *a* according to the stoichiometric values shown in Table 1. The ideal situation sketched would correspond to a PHEA molecular mass between cross-links equal to $M_{PHEA} = \frac{1}{2}\frac{n_{HEA}}{n_{mLA}} M_{HEA}$. The average molar mass of the network between cross-links can be calculated according to the model sketched in Fig. 11, taking into account the functionality of the ideal joint as,

$$M = \frac{2}{3} M_{PHEA} + \frac{1}{3} M_{mLA} \tag{5}$$

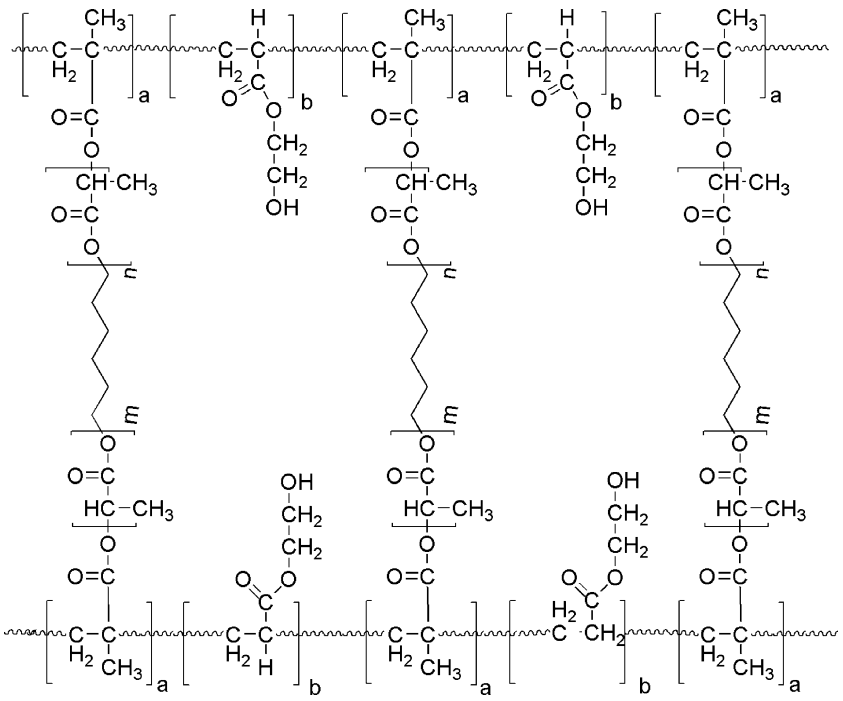

Fig. 11 Sketched copolymer networks as suggested by the stoichiometric ratios of the comonomers and the physicochemical characterization. The number units of HEA between cross-links "*a*" are shown in Table 1

Table 1 shows the calculated values according to the previous equation. Following the theory of rubber elasticity, the molar concentration n_c/V of elastically active or effective chains is related to the rubber modulus [42] by

$$E' = 3A_\phi \frac{n_c}{V} RT = 3A_\phi \frac{d}{M_c} RT \quad (6)$$

where R is the universal gas constant, d is the density, T is the absolute temperature, E' is the modulus in the elastomeric region at T, M_c is the average molar mass between cross-links, and A_ϕ is a factor that depends on how much the deformation deviates from the affine limit, in which the displacements of the cross-links are a simpler linear function of the macroscopic strain. For the non-affine "phantom" network model, the theory indicates

$$A_\phi = 1 - \frac{2}{\phi} \quad (7)$$

with ϕ as the functionality of the knot in the network. For our networks (Fig. 11), ϕ=3, and M_c can be calculated from the experimental E' values in the rubbery region; the data and the results are shown in Table 1.

The molar mass between cross-links *p*(mLA) network is much higher (M~14,000) than the molecular weight of the macromonomer mLA used as the base material for the synthesis of the network (M~3,500). This fact suggests that *p*(mLA) network contains a number of dangling chains due to the lack of connectivity of the whole network. That is to say, the *p*(mLA) homonetwork is rather imperfect as compared with the ideal, perfectly connected one, sketched in Fig. 11 (with b=0). This is also correlated with the much higher specific volume of the *p*(mLA) network compared with the rest of copolymers. Moreover, predictions of Eq. 6 are consistent with the expected-ideal values from stoichiometry for the rest of copolymer, which suggests, on the one hand, that the proposed ideal model shown in Fig. 11 is a reasonable physical picture of the actual copolymer networks and, on the other hand, that the lower amounts of HEA in the copolymer (13 HEA units per mLA chain) are able to interconnect the dangling mLA chains.

Concluding, the development of the new system allows cross-linking polylactide and its hydrophilizaton by copolymerization with hydrophilic units (HEA). The existence of both hydrophilic and hydrophobic domains must improve protein adsorption and cell adhesion [43, 44], increasing the wettability and the transport of active molecules. However, the formation of a network modifies the mechanical properties of the system, which could have an influence in protein adsorption [45–47]. Based on this system, we are currently preparing scaffolds with well-defined pore structure that can be utilized as supports in tissue engineering applications.

Conclusions

A method for obtaining photo-cross-linkable mLA macromer is described. Copolymer networks of the mLA macromer and hydrophilic hydroxyethyl acrylate monomer can be synthesized by free radical polymerization in order to tailor the water-uptake of the system. The new system is mechanically stable and consists of phase-separated microdomains richer in one or the other comonomers that constitute the network. The architecture of the copolymer networks is suggested to be that of a network with trifunctional joints in which two branches consist of PHEA (of varying length depending on the weight fraction of HEA in the monomers mixture) and the other of *p*(mLA) macromer as supported by the prediction of the phantom theory of rubber elasticity.

Acknowledgments The support of the Spanish Ministry of Science through project No. MAT2006-08120 (including the FEDER financial support) is kindly acknowledged. JLEI acknowledges Generalitat Valenciana for the support through the predoctoral grant CTBPRB/2005/075.

Appendix

Short text for the table of contents

A new set of copolymer networks based on poly(L-lactide) macromer *p*(mLA) was synthesized, whose water sorption behavior can be modulated by copolymerization with a hydrophilic monomer. The new block copolymer network is able to tailor the water sorption capacity, keeping the *p*(mLA) properties. The figure shows the ideal structure for the hydrophilized *p*(L-lactide) networks.

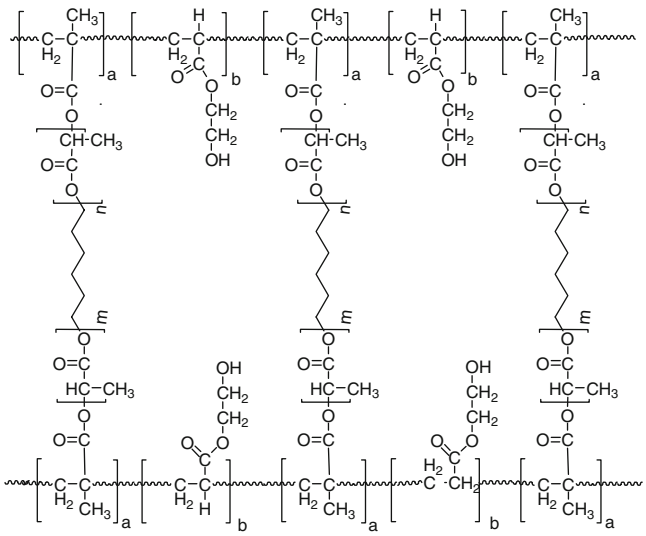

References

1. Langer R, Vacanti JP (1993) Science 260:920
2. Peppas NA, Langer R (2004) Aiche J 50:536
3. Jagur-Grodzinski J (2006) Polym Adv Technol 17:395
4. Lavik E, Langer R (2004) Appl Microbiol Biotechnol 65:1
5. Cao Y, Carol TI (2005) Aust J Chem 58:691
6. Wang YK, Yong T, Ramakrishna S (2005) Aust J Chem 58:704
7. Grijpma DW, Pennings AJ (1994) Macromol Chem Phys 195:1633
8. Holland SJ, Tighe B, Gould PLJ (1986) J Control Release 4:155
9. Vert M, Li SM, Spenlehaur G, Guerin P (1992) J Mater Sci Mater Med 3:432
10. Vert M, Schwarch G, Coudane J (1995) J Macromol Sci Pure Appl Chem A32:787
11. Kharas GB, Kamenetsky M, Simantirakis J, Beinlich KC, Rizzo AMT, Caywood GA, Watson K (1997) J Appl Polym Sci 66:1123
12. Peter SJ, Kim P, Yasko AW, Yaszemski MJ, Mikos AG (1999) J Biomed Mater Res 44:314
13. Domb AJ, Manor N, Elmalak O (1996) Biomaterials 17:411
14. Kim BS, Hrkach JS, Langer R (2000) J Polym Sci Part A: Polym Chem 38:1277
15. Burdick JA, Mason MN, Anseth KS (2001) J Biomater Sci Polym Ed 12:1253
16. Burdick JA, Padera RF, Huang JV, Anseth KS (2002) J Biomed Mater Res 63:484
17. Horbett TA, Schway MB, Ratner BD (1985) J Colloid Interface Sci 104:28
18. Horbett TA, Schway MB (1988) J Biomed Mater Res 22:763
19. Chinn JA, Horbett TA, Ratner BD, Schway MB (1989) J Colloid Interface Sci 127:67
20. Ertel SI, Ratner BD, Horbett TA (1990) J Biomed Mater Res 24:1637
21. Muller M, Oehr C (1999) Surf Coatings Technol 116:802
22. Klee D, Villari RV, Hocker H, Dekker B, Mittermayer C (1995) J Mater Sci Mater Med 5:592
23. Fang YE, Lu XB, Wang SZ, Zhao X, Fang F (1996) J Appl Polym Sci 62:2209
24. Ajayaghosh A, Das S (1992) J Appl Polym Sci 45:1617
25. Geuskens G, Etoc A, Michele PD (2000) Eur Polym J 36:265
26. Kang IK, Kwon BK, Lee JH, Lee HB (1993) Biomaterials 14:787
27. Lee JS, Kaibara M, Iwaki M, Sasabe H, Suzuki Y, Kusakabe M (1993) Biomaterials 14:958
28. Sato H, Tsuji H, Ikeda S, Ikemoto N, Ishikawa J, Nishimoto S (1999) J Biomed Mater Res 44:22
29. Park TG, Cohen S, Langer R (1992) Macromolecules 25:116
30. Barakat I, Dubois PH, Grandfils CH, Jérôme R (1999) J Polym Sci Part A: Polym Chem 37:2401
31. Grijpma DW, Pennings AJ (1991) Polym Bull 25:335
32. Grijpma DW, Zondervan GJ, Pennings AJ (1991) Polym Bull 25:327
33. Albertsson AC, Gruvegard M (1995) Polymer 36:1009
34. Jamshidi K, Hoyn SH, Ikada Y (1988) Polymer 29:2229
35. Hoyn SH, Jamshidi K, Ikada Y (1997) Biomaterials 18:1503
36. Escobar Ivirico JL, Salmerón Sánchez M, Sabater i Serra R, Meseguer Dueñas JM, Gómez Ribelles JL, Monleón Pradas M (2006) Macromol Chem Phys 207:2195
37. Escobar Ivirico JL, Costa Martínez E, Salmerón Sánchez M, Criado Muñoz I, Gómez Ribelles JL, Monleón Pradas M (2007) J Biomed Mater Res. Part B Appl Biomat 83B:266
38. Tutusaus O, Delfosse S, Simal F, Demonceau A, Noels AF, Núñez R, Viñas C, Teixidor F (2002) Inorg Chem Commun 5:941
39. Kanaoka S, Sawamoto M, Higashimura T (1991) Macromolecules 24:2309
40. Salmerón Sánchez M, Gómez Ribelles JL, Hernández Sánchez F, Mano JF (2005) Thermochim Acta 430:201
41. López-Rodríguez N, López-Arraiza A, Meaurio E, Sarasua JR (2006) Polym Eng Sci 9:1299
42. Flory PJ (1953) Principles of polymer chemistry. Cornell University Press, Ithaca
43. Arima Y, Iwata H (2007) Biomaterials 28:3074
44. Marchin KL, Berrie CL (2003) Langmuir 19:9883
45. Pelham JR, Wang YL (1997) Proc Natl Acad Sci U S A 94:13661
46. Gray DS, Tien J, Chen CS (2003) J Biomed Mater Res 66A:605
47. Genes NG, Rowley JA, Mooney DJ, Bonassar LJ (2004) Arch Biochem Biophys 422:161